

# Golf Analytics: A Random Putting Model and its Applications to Optimal Targeting Strategy and Attribution Analysis

Mark Broadie  
Graduate School of Business  
Columbia University  
email: mnb2@columbia.edu

Dongwook Shin  
Graduate School of Business  
Columbia University  
email: dshin17@gsb.columbia.edu

October, 2014

## Abstract

Golf analytics is the study of data to discover patterns and opportunities that enable the creation of decision support systems in golf, incorporating analytically based simulation and optimization technologies. In this paper we use the PGA Tour data from the ShotLink system to infer putting performance statistics as a function of putt length, angle, and slope. Contrast to the existing studies that rely on the relationship between the putting performance statistics and putt length only, we infer interesting features in the data for different putt angles and slopes. Motivated by the patterns observed in the data, we develop and validate a random trajectory model and calibrate it for use in simulation. Based on the calibrated model we numerically find optimal target distance beyond hole as a function of putt length, angle, and slope, and suggest how much one can expect to improve putting performance by adopting the optimal targeting strategy, without improving intrinsic putting skills. Lastly, we perform an attribution analysis to evaluate what putting skill is most critical to the performance.

## 1. Introduction

**Background and motivation.** Putting is a separate game within the game of golf. According to the PGA tour data from 2003 to 2010, putting accounts for 40% of the strokes taken and 15% of the variation in scores (Broadie, 2012). This means that a golfer has an ample opportunity to make the better results in tournaments by improving putting performance. The patterns and linkages observed in data enable us to identify strengths and weaknesses of a golfer and to build a strategy to achieve the best-possible result. We use the PGA Tour data from the Shotlink system, which we turned into useful knowledge by inferring descriptive statistics from the data.

To develop the knowledge into a strategic decision in putting, we model a trajectory of a ball on green by adding randomness to a deterministic trajectory model in physics. This random trajectory model, combined with simulation and optimization techniques, is an ideal tool for making a strategic decision in putting for the following reasons. First, simulation is generally cheaper and safer than conducting experiments on real green. It would take a lot of money and effort to collect empirical data from professional or amateur golfers because of the limited budgets in space and time, whereas numerical experiment using simulation provides immediate results. Also, simulation is more flexible

in terms that one can control the details of the model using parameters, such as putting skill levels, targeting strategy, and other environmental factors.

**Literature review.** Research on the physics model for a ball trajectory on green has been pursued in many literature. The trajectory model in Vanderbei (2001) is the simplest model in terms that the following aspects are ignored. First, a ball trajectory on green consists of both skidding and rolling phases, which makes it hard to build an exact physics model. Second, the green grass is deformed as a ball moves on the surface. Hence, a ball trajectory on green is different from that on a solid surface. Perry (2002) developed the Vanderbei’s model by considering the sliding and rolling effects. Penner (2002) introduced the concept of the *retarding force* which is caused by the deformed green surface, and derived the equations for a trajectory, assuming the ball moves without skidding.

Holmes (1991) studies the encounter of a rolling golf ball with a hole; he derived conditions for holeout in the following two cases: (1) a ball directed toward the center of the hole; and (2) a ball directed off-center. Penner (2002) developed a simple condition for holeout; this is an approximate, but fairly accurate condition for holeout in terms that it matches well with the experimental measurements that Holmes carried out. In this paper we use the trajectory and the holeout model in Penner (2002).

The aforementioned trajectory models are deterministic; that is, the trajectory of a putt is a deterministic function of launch velocity and direction. Gelman and Nolan (2002) introduced a random putting model where the launch direction is random—hence, the trajectory is also random. Bansal and Broadie (2008) generalized the random putting model in which three sources of randomness are concerned: errors in launch direction, launch velocity, and reading green slope. The direction and velocity errors occur because a golfer cannot hit the ball exactly at the intended direction and velocity, while the green reading error occurs because a golfer cannot read the exact slope of a green. Although some external factors, such as wind, humidity, and irregularity on green grass, can make the trajectory more unpredictable, these factors are ignored in this paper because they have negligible effects compared to the three random factors in Bansal and Broadie (2008).

A targeting strategy is also studied in putting literature. A target distance is the distance from a hole to an imaginary target point a golfer aims; the ball would stop at the target point if the hole were covered. Pelz (2000) has examined the optimal target distance by an empirical experiment with a rolling device, and suggested 1.5 feet beyond hole as an optimal target. Although the constant target distance is an appealing strategy in practice, we acknowledge that the result of the experiment with the device cannot be generalized to golfers and develop more delicate targeting strategy in Section 4.2.

**Main contributions.** This paper makes four main contributions.

- *We infer putting performance statistics as functions of putt length, angle, and slope.* Using the Golfmetrics software (Broadie, 2008), we study the big data collected in the Shotlink system and discover patterns in putting performance statistics, such as average number of putts, one-putt probability, three-putt probability, fraction short, and standard deviation of remaining distances.

Especially, we highlight the relationship between the putting statistics and putt angle, e.g., downhill, sidehill, and uphill, since it is less studied in detail in the putting literature.

- *We calibrate the random putting model to the data.* We first show that random putting models that only consider physical putting skills (i.e., direction and velocity errors) are not appropriate since they generate the opposite putt-angle patterns than those observed in the data. In particular, we validate that the model by Bansal and Broadie (2008), which considers additional green-reading factor, in the sense that it replicates such patterns correctly. We find least-squares estimators for a set of parameters for the random putting model to match the weighted sum of putting performance statistics from the data. The parameters include those for the physical factors, green reading factor, as well as a targeting strategy. In the previous literature, the target distance is fixed to a constant value (e.g., 1.5 feet beyond the hole), whereas we consider it as a parameter to be fitted. It will be shown in Section 4 that the calibrated target distance significantly varies by putt length, angle, and slope; it is far from a constant value.
- *We numerically find an optimal targeting strategy.* We use the calibrated model to derive an optimal targeting strategy, i.e., optimal target distance beyond hole as a function of putt length, angle, and slope. We conclude that an aggressive target generally improves performance. Further, we perform a numerical experiment with the optimal targets, and discuss how much one can lower the putting score with the optimal targeting tactic, without improving intrinsic putting skills.
- *We study what factor is most critical in the putting performance.* According to the data, the difference in putts per round between the best and worst putters among the professional golfers is about 1.6, where the definitions of the best and the worst putters are given in Section 2. We decompose this gap by four factors: the difference due to direction error, velocity error, green reading error, and suboptimal fraction-short strategy. It turns out that the green-reading and the direction control abilities are the key factors for the better performance, while the distance control ability (i.e., velocity error and fraction short strategy) has minor impact on it.

**Remainder of the Paper.** In Section 2 we explain how the data is collected and manipulated to infer the putting performance statistics as functions of putt length, angle, and slope. Some patterns in the data will be illustrated in detail. In Section 3, we review a green model and a deterministic trajectory model, from which we develop a random putting model. In Section 4, the calibration result is provided. Also, some implications from numerical experiments will be discussed; in particular, we discuss the optimal targeting strategy in Section 4.2 and perform an attribution analysis in Section 4.3. The detailed methods on numerical experiments is discussed in the Appendix.

## 2. Data

**Processing data.** We use the putting data collected in the Shotlink system, which contains approximately 4 million number of putts in PGA Tour events. In the ShotLink system, each golf

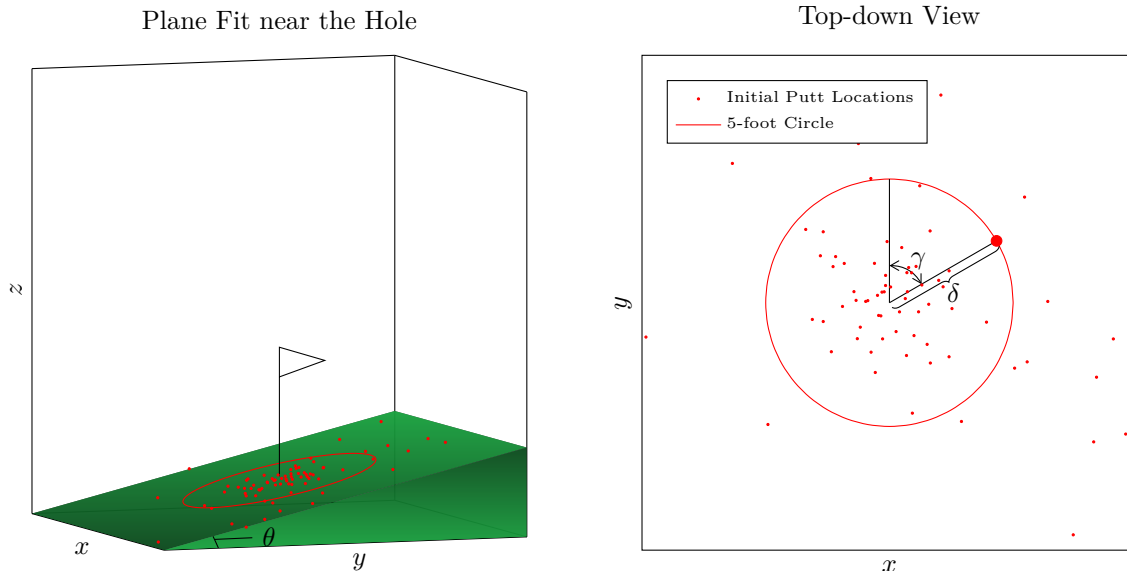


**Figure 1:** On the left panel, the red dots represents the initial putt positions from ShotLink data on one of the greens in Congressional Country Club, Maryland, USA. The planar surface is fitted to the putts that are within 5-foot from the hole by solving (1). The scale in  $z$ -axis is enlarged for a better illustration. Each red dots is projected onto the fitted planar surface, and the putt position is expressed as a 3-tuple; putt length ( $\delta$ ), angle ( $\gamma$ ), and slope ( $\theta$ ).

course is mapped as a digital image to record 3-dimensional coordinates of a golf ball. To be specific, it records the following information of each putt: the name of the golfer, the name of the golf course, the hole number, the  $xyz$ -locations of the initial and end position of a ball, hole location, the number of putts to holeout, and an indicator whether it is the first putt or not. In this section we sketch how we process the data from which we infer performance statistics. Note that as opposed to the performance statistics for *individual* golfers, we are interested in the *aggregate* performance statistics at different putt locations.

First, we fit each green to a flat surface. Generally, green is almost flat around the hole, say, within 5 feet from the hole. For a particular green, suppose that we have  $N$  points within 5 feet from the hole. These  $N$  points are either initial or end positions of putts. Denote each point as  $(x_n, y_n, z_n), n = 1, \dots, N$ . In the three-dimensional coordinate a flat surface is characterized by four coefficients, i.e.,  $\{(x, y, z) \mid ax + by + cz + d = 0\}$ . We fit the green to a flat surface by finding the coefficients,  $(\hat{a}, \hat{b}, \hat{c}, \hat{d})$ , such that the sum of squared distances from the  $N$  points to a plane,  $\{(x, y, z) \mid \hat{a}x + \hat{b}y + \hat{c}z + \hat{d} = 0\}$  is minimized. Formally,

$$(1) \quad (\hat{a}, \hat{b}, \hat{c}, \hat{d}) = \underset{(a,b,c,d) \in \mathcal{R}^4}{\operatorname{argmin}} \sum_{n=1}^N \left( \frac{ax_n + by_n + cz_n + d}{\sqrt{a^2 + b^2 + c^2}} \right)^2$$

By solving the optimization problem for each green, we obtain a unique flat surface  $\{(x, y, z) \mid \hat{a}x + \hat{b}y + \hat{c}z + \hat{d} = 0\}$ . This allows us a simple representation of each green with only a few parameters.

Second, we translate each initial putt location in the  $xyz$ -coordinate into 3-tuple; distance from

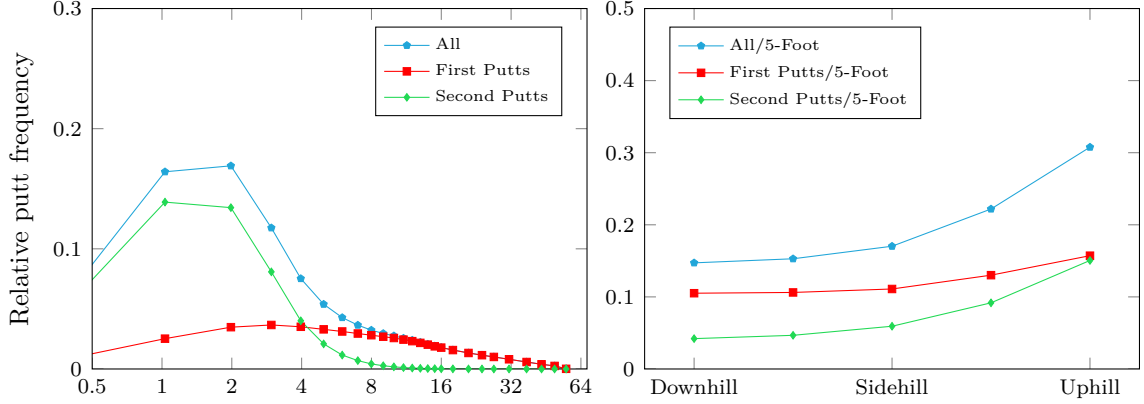


**Figure 2:** Relative putt frequency from data by putt length (left) and by putt angle (right). The second putts are concentrated on short-length putts, while the first putts are evenly distributed over the putt length. On the right panel, it is interesting to note that the uphill putts are more frequent than equidistant downhill putts, which indicates professional golfers’ tendency to approach to “uphill” position than to “downhill” position so as to make the next putt easier.

the hole to the initial location (putt length,  $\delta$ ), angle from the fall line (putt angle,  $\gamma$ ), and inclination of the green (slope,  $\theta$ ). The translation is straightforward from the illustration in Figure 1; first, project each point  $(x_n, y_n, z_n)$  on to the plane,  $\{(x, y, z) \mid \hat{a}x + \hat{b}y + \hat{c}z + \hat{d} = 0\}$ , and denote the projected point as  $(\hat{x}_n, \hat{y}_n, \hat{z}_n)$ . Then, looking at the relative location of  $(\hat{x}_n, \hat{y}_n, \hat{z}_n)$  to the hole, the putt length, angle, and slope for each projected point are obtained after some simple algebra. Note that this is a *relative* location to the hole; for example, a putt location,  $(\delta, \gamma, \theta)$ , on green A is considered the same location as  $(\delta, \gamma, \theta)$  on a different green B. This allows us to aggregate the putt data across all greens.

Third, the putt locations are pooled into groups. To be specific, we divide the plane into  $K$  distinct sub-planes, where each sub-plane is represented by a point,  $I_k = (\delta_k, \gamma_k, \theta_k), k = 1, \dots, K$ . Then, every (actual) putt location is classified as one of the  $K$  locations closest to itself. The frequency of putts for each category is summarized in Figure 2.

As a last step, we infer performance statistics from the pooled data. For each putt, by looking at the initial and end locations, along with the hole location, it is possible to infer whether it is holeout or not. If it misses the hole, we can infer how long the remaining distance from the hole is. Further, we can deduce whether the putt is short to the hole or not. We aggregate all these results within each category  $I_k, k = 1, 2, \dots, K$  to derive the following performance statistics.

- Average number of putts: the average of the number of putts until holeout
- One-putt probability (resp. three-putt probability): the probability that a ball is holeout in one shot (resp. in three shots)
- Fraction short: the relative frequency of putts for which the distance from the initial to the end position is less than the distance from the initial position to the hole
- Standard deviation of remaining distance: the standard deviation of the distances from the

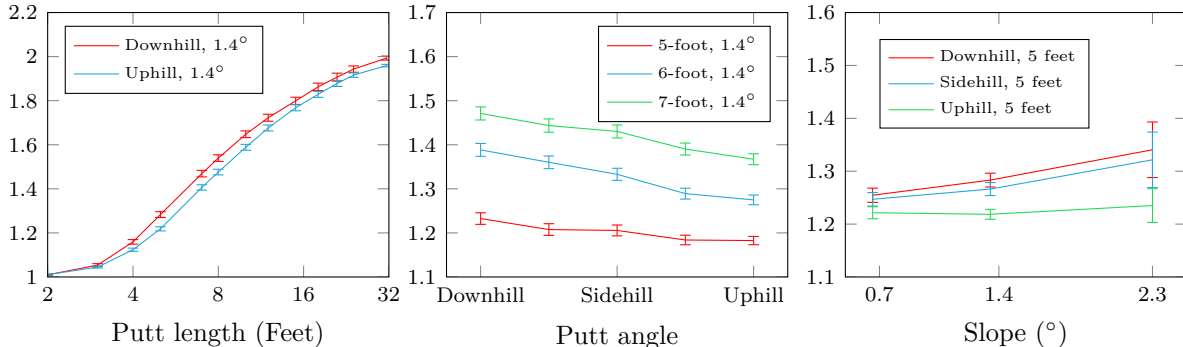


**Figure 3:** Average number of putts for *average* putter from PGA Tour’s Shotlink data. Each vertical error bar is 95% confidence interval about each estimation. Average number of putts increases with putt length and slope, and is higher for downhill putts than equidistant uphill putts.

hole to the end position of missed putts.<sup>1</sup>

These performance measures are obtained for each putt location  $I_k$ , hence, they are effectively (discrete) functions of putt length, angle, and slope.

**Patterns in performance statistics.** Some relationships between the performance statistics and putt length are studied in Broadie (2008), yet here we provide additional, important patterns in the data for different putt angles and slopes. Representatively, the average number of putts are shown as a function of putt length, angle, and slope in Figure 3. As expected, the average number of putts increases with putt length and slope, as shown in the left and the right panels in Figure 3. However, the putt-angle patterns in the middle is not straightforward. One might argue that the putt-angle pattern should be upwardly sloping because the trajectory of a downhill putt tends to be curved toward the hole due to the gravity, while the trajectory of an uphill putt tends to be curved away from the hole, it may seem that the downhill putt is easier than the uphill. However, as the putt-angle pattern in Figure 3 suggests, downhill putts are actually harder than the equidistant uphill putts. This pattern will be explained in detail later in Section 3.4.

**Best, Average, and Worst Putters.** We divide PGA Tour golfers into three groups: the best, average, and worst putters, according to their putting performance. Specifically, the best putter gains 0.5 putts per round on an annual basis compared to the average putter, while the worst putter loses 0.5 putts per round. See Figure 15 in the appendix for the average number of putts data for the three groups of putters. According to the data, the numbers of putts per round are 28.4, 29.2, 30.0 for the best, average, and worst putters, respectively. In Section 4.3 we examine what factor drives the gap between the best and the worst putters in detail.

**First and Second putts.** The Shotlink data are further divided into two types of putts: the first and the second putts. As the name suggests, the second putt is defined as the putt whose previous shot has missed the hole. To take into account the fact that the second putts are generally closer to a hole than the first putts, we use different notations for the first and the second putts.

<sup>1</sup>Standard deviation of remaining distance is the statistics for missed putts, while the other statistics are for all putts.

We let  $I_k = (\delta_k, \gamma_k, \theta_k)$ ,  $k = 1, 2, \dots, K$ , denote locations for the first putts and let  $I'_k = (\delta'_k, \gamma'_k, \theta'_k)$ ,  $k = 1, 2, \dots, K'$ , denote locations for the second putts.  $\delta_k$  ranges from 1 to 68 feet, while  $\delta'_k$  ranges from 1 to 18 feet. Throughout the paper, we use the same sets of putt angle and slope for both types of putts, i.e.,  $\{\gamma_k\} = \{\gamma'_k\}$  and  $\{\theta_k\} = \{\theta'_k\}$ . See Figure 14 in the appendix for the performance statistics for the two types of putts.

**Remark on the notation.** Throughout the paper we use calligraphic  $\mathcal{I} = \mathcal{I}(\delta, \gamma, \theta)$  to denote putt location in continuous spaces, and  $I_k = I(\delta_k, \gamma_k, \theta_k)$  to denote discrete putt location as defined in this section.

### 3. Model

#### 3.1. Green Model

We model a green as a perfectly flat, sloped surface. In particular, we ignore any inconsistencies on the green surface that are caused by external forces such as footprints left by golfers and improperly repaired grass. These assumptions on greens are mild and reasonable, given the fact that greens are well-maintained in PGA Tour events. The flat green is characterized by slope and speed. The slope is the degree of inclination of the planar green surface, quoted as a degree ( $^\circ$ ). Since the green is planar, the slope is constant on the entire green surface. The speed is characterized in terms of the Stimp speed of the green. The Stimp speed is the distance measured in feet that a golf ball rolls when launched from a Stimp device on a level surface. The greens with large Stimp speed, e.g. 14-Stimp speed, are called fast greens and the greens with small Stimp speed, e.g. 8-Stimp speed are called slow greens. In the model, we assume that the green speed is constant and is 11-Stimp, the average green speed in the PGA Tour events.

To be consistent with the notation in the data in Section 2, a putt location on a green is jointly represented by putt length, angle, and slope, i.e.,  $\mathcal{I} = (\delta, \gamma, \theta)$ . Since the green is in three-dimensional space, the slope of a surface is a pair,  $\theta = (\theta_x, \theta_y)$ , where  $\theta_x$  (resp.  $\theta_y$ ) is the slope of the green with respect to  $yz$ -surface (resp.  $xz$ -surface). For a simple notation, we sometimes use a scalar  $\theta_y$  to represent the slope, in which case  $\theta_x$  is set to 0. In our context, downhill, sidehill, and uphill putts correspond to putt angles  $0^\circ$ ,  $90^\circ$ , and  $180^\circ$ , respectively.

#### 3.2. Trajectory and Holeout Models

The motion of the golf ball on a sloped green surface is more involved than it appears to be. Unlike the movement of a ball on a solid surface, the golf ball deforms the green surface while moving and the magnitude and the direction of the *retarding force* are affected by this deformation. We make a simplifying assumption that a golf ball rolls without skidding, and the differential equations for a trajectory of a purely rolling ball on a planar green surface have been developed by Penner (2002). We omit the derivation of those equations, but briefly explain the numerical integration method to solve the sequence of differential equations in Appendix A.1. We define the trajectory of a putt

$\mathcal{T} \equiv \mathcal{T}(v, \alpha; \mathcal{I})$  as a function of  $(v, \alpha)$ , a pair of launch velocity and direction<sup>2</sup>, given putt location  $\mathcal{I} = (\delta, \gamma, \theta)$ .

Holmes (1991) studied the problem of the capture of a golf ball by a hole on a planar surface. The ball at the edge of the hole can be captured by the hole in several ways. For example, it could just free-fall into the hole directly, hit the far edge of the hole, or roll along the rim of the hole before dropping into the hole. Taking into account all these possibilities, Penner (2002) derived a very simple condition for holeout as a function of an impact speed and an impact parameter<sup>3</sup>. We adopt the Penner’s holeout model but omit the detail because it is not in the scope of this paper.

### 3.3. Target Distance and Launch Conditions

In a putting situation, a golfer sets an imaginary target point beyond the hole and decides launch velocity and direction, expecting that it would stop at the target point if the hole were covered. For each putt location  $\mathcal{I}$ , we denote  $d(\mathcal{I})$  as a target distance, the distance from the center of the hole to the target point. We call a vector of target distances  $D$  as a targeting strategy, i.e.,  $D = (d(I_1), \dots, d(I_K), d'(I'_1), \dots, d'(I'_K))$ , where  $d'(I'_k)$  implies the target distance for the second putt at the location  $I'_k$ .

Holeout region is a range of a pair of launch velocity and direction that would lead to holeout. See Figure 4 for a 10-foot sidehill putt as an example. Among all pairs in the holeout region, we call  $(v_d, \alpha_d)$  a *target* launch condition for the target distance  $d$ . There is a unique pair,  $(v_d, \alpha_d)$ , for each target distance  $d$ ; for example, in Figure 4,  $(v_d, \alpha_d)$  is the unique point in a holeout region at which the trajectory  $\mathcal{T}(v_d, \alpha_d; \mathcal{I})$  would cross the center of the hole and stop  $d$  feet beyond the hole, if the hole were covered.

### 3.4. Random Trajectory Model

Now we are ready to build a random trajectory model for putting. The core of our model is the routine for generating random result of a single putt given an initial position on a green surface and a target distance beyond hole. To start, we introduce three sources of randomness: randomness in reading green slope, in launch direction, and in launch velocity. We refer to these errors as green reading error, direction error, and velocity error, respectively. The combination of these sources of errors results in random launch velocity and direction—hence, a random trajectory. In this subsection, we fix the target distance  $d$  and putt location  $\mathcal{I}$ , and illustrate how to generate a random trajectory given  $d$  and  $\mathcal{I}$ .

*The green reading error* occurs because golfers cannot perfectly read the slope of a green. Suppose that the true slope of green is given as  $\theta = (\theta_x, \theta_y)$ . Then a golfer’s (random) estimate of

---

<sup>2</sup>Velocity is measured in m/s and direction is measured in degrees. The positive direction indicates that a golfer aims right side of the hole, and the negative direction indicates that a golfer aims left side of the hole.

<sup>3</sup>The impact speed is the speed of the ball at the rim of a hole, and the impact parameter is the perpendicular distance from the center of a hole to the direction of the ball at the rim.

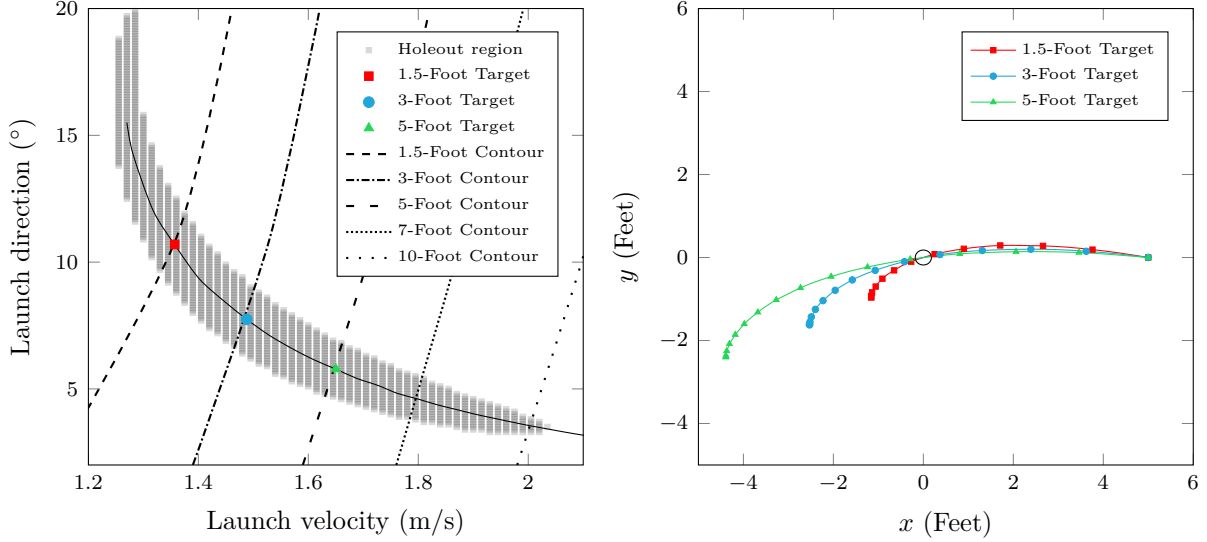


**Figure 4:** The hole out region for a 10-foot sidehill putt on  $2.0^\circ$ -sloped green, i.e.,  $\mathcal{I} = (10 \text{ feet}, 90^\circ, 2.0^\circ)$ . The gray area is the holeout region, the solid line that cuts the holeout region by half is the pair  $(v, \alpha)$  at which the ball goes through the center of the hole, and the dotted and the dashed lines are contour lines for distance beyond the hole. In the right panel there are three trajectories with the target 1.5 feet, 5 feet, and 9 feet beyond hole, respectively. For instance, the  $(v_{1.5}, \alpha_{1.5})$  is the red square marker on the left panel at which the 1.5-foot contour line and the solid line intersects, and the red trajectory on the right panel corresponds to the launch condition,  $(v_{1.5}, \alpha_{1.5})$ .

the slope  $\hat{\theta} = (\hat{\theta}_x, \hat{\theta}_y)$  is generated by a polar method:

$$(2) \quad \begin{aligned} \hat{\theta}_x &= \theta_x + r \cos \phi \\ \hat{\theta}_y &= \theta_y + r \sin \phi, \end{aligned}$$

where  $r \sim N(0, \sigma_g^2)$  and  $\phi \sim Unif(0, 2\pi)$ . In a putting situation, a golfer determines the target velocity and direction based on his/her estimate  $\hat{\theta}$ , instead of the true slope  $\theta$ . We let  $\hat{\mathcal{I}}$  be the putt location with erroneous green estimate, i.e.,  $\hat{\mathcal{I}} = (\delta, \gamma, \hat{\theta})$ , whereas the true location is  $\mathcal{I} = (\delta, \gamma, \theta)$ .

Our model allows that the estimated green slope at the second putt can be different from the initial estimate because a golfer updates the green slope after observing the trajectory of the first putt. To take into account the different green reading skills, we denote  $\sigma_{g1}$  and  $\sigma_{g2}$  as the green reading errors for the first and the second putts, respectively. Note that the green reading error is parameterized by  $(\sigma_{g1}, \sigma_{g2})$ .

*The direction error* occurs because golfers cannot hit the ball exactly at the intended direction. We assume that launch direction  $\alpha$  is normally distributed with mean  $\alpha_d$  and standard deviation  $\sigma_\alpha$ :

$$(3) \quad \alpha \sim N(\alpha_d, \sigma_\alpha^2),$$

where  $\alpha_d$  is uniquely determined for the target distance  $d$  at the location  $\hat{\mathcal{I}}$ , as illustrated in the



**Figure 5:** Direction error v.s. green reading error. These are 12-foot straight downhill and uphill putts on  $1.5^\circ$ -sloped green with the fall line along  $y$ -axis, i.e.,  $\theta = (0^\circ, 1.5^\circ)$ . The target distance is 1.5 feet beyond the hole. The  $x$ -axis is magnified 3 times for better illustration; in the above figures,  $x$ -axes range from -4 to 4 feet, while  $y$ -axes range from -12 to 12 feet. In the left panel, the direction error is  $\pm 2^\circ$  and the green reading error is 0. In the right panel, the direction error is 0 and the green reading error is  $\pm 0.5^\circ$  along  $x$ -axis, i.e.,  $\hat{\theta} = (\pm 0.5^\circ, 1.5^\circ)$ . In the right panel, the target direction for downhill putts is  $\bar{\alpha} = \pm 4.1^\circ$ , while it is  $\bar{\alpha} = \pm 1.8^\circ$  for uphill putts.

subsection 3.3. It is important to note that the target direction is determined at  $\hat{\mathcal{I}}$ , not at the true location  $\mathcal{I}$ . Note that the direction error is parameterized by  $\sigma_\alpha$ .

As briefly mentioned in Section 2, it is important to note that green reading error and direction error have very different effects. The direction error makes uphill putts harder than equidistant downhill putts, while the green reading error makes the opposite effect. Specifically, suppose there is no green reading error and the magnitude of direction error (i.e.,  $|\alpha - \alpha_d| > 0$  in (3)) is the same for uphill and downhill putts. Due to gravity, the downhill putt would be curved into the hole, while the uphill putt would be curved away from the hole (See the left panel of Figure 5). Hence, the downhill putt is easier than the uphill putt in this case. Conversely, suppose there is no direction error and the magnitude of the green reading error (i.e.,  $|r| > 0$  in (2)) is the same for uphill and downhill putts. In this case, for each putt location  $\hat{\mathcal{I}}$ ,  $\alpha = \alpha_d(\hat{\mathcal{I}})$  since there is no direction error in (3). However,  $\alpha_d(\hat{\mathcal{I}})$  is affected by the green reading error; indeed, from the right panel of Figure 5, it can be seen that  $|\alpha_d(\hat{\mathcal{I}}) - \alpha_d(\mathcal{I})|$  is greater for the downhill putt than for the uphill putt. Hence, unlike the first case, the downhill putt is harder than the uphill putt when there is some green reading error.

The *velocity error* occurs because golfers cannot hit the ball exactly at the intended target velocity. We give randomness to  $v^2$ , not to  $v$  itself.<sup>4</sup> We assume that the squared velocity  $v^2$  is

<sup>4</sup>The total length of a putt trajectory is approximately proportional to  $v^2$ , not to  $v$ . This is the reason why the model with  $v^2$ -error is preferred to the one with  $v$ -error.

normally distributed with mean  $v_d^2$  and standard deviation  $f(v_d^2)$ :

$$(4) \quad v^2 \sim N(v_d^2, f^2(v_d^2)).$$

$v_d$  is the target distance uniquely determined for the target distance  $d$  at the location  $\hat{\mathcal{L}}$ . Note that, unlike the direction error, the standard deviation of  $v^2$ ,  $f(\cdot)$ , is a function of the squared target velocity  $v_d^2$ . Intuitively, the harder the ball is hit, the more deviation in launch velocity. Therefore, we allow the standard deviation of  $v^2$  to be a function of  $v_d^2$ . In particular, we model  $f(\cdot)$  as a continuous, non-negative, piecewise linear function with  $k$  break points,  $v_i^2$ ,  $i = 1, \dots, k$ , i.e.,

$$(5) \quad f(v_d^2) = \begin{cases} \sigma_{v_1^2} + (v_d^2 - v_1^2)(\sigma_{v_2^2} - \sigma_{v_1^2})/(v_2^2 - v_1^2) & , \text{ for } v_d < v_1, \\ \sigma_{v_{i-1}^2} + (v_d^2 - v_{i-1}^2)(\sigma_{v_i^2} - \sigma_{v_{i-1}^2})/(v_i^2 - v_{i-1}^2) & , \text{ for } v_{i-1} \leq v_d < v_i, i = 2, \dots, k, \\ \sigma_{v_{k-1}^2} + (v_d^2 - v_{k-1}^2)(\sigma_{v_k^2} - \sigma_{v_{k-1}^2})/(v_k^2 - v_{k-1}^2) & , \text{ for } v_k \leq v_d. \end{cases}$$

For completeness, we let  $v = 0$  if the generated  $v^2$  is negative, though such a truncation is rarely needed in practice. Note that the velocity error is parameterized by  $k$  values,  $\sigma_{v_1^2}$ ,  $\sigma_{v_2^2}$ , and  $\sigma_{v_k^2}$ .

To wrap up, a random trajectory  $\mathcal{T}(v, \alpha; \mathcal{I}, d)$  is simulated as follows:

*Step 1.* (Generate green reading error) Given the true slope  $\theta = (\theta_x, \theta_y)$ , draw random vector  $\hat{\theta} = (\hat{\theta}_x, \hat{\theta}_y)$  from (2) and let  $\hat{\mathcal{L}} = (\delta, \gamma, \hat{\theta})$ .

*Step 2.* (Compute target launch conditions) For the given target distance  $d$ , compute  $(v_d, \alpha_d)$  at the putt location  $\hat{\mathcal{L}}$  in *Step 1*.

*Step 3.* (Generate direction and velocity errors) Given  $(v_d, \alpha_d)$  in *Step 2*, draw random vector  $(v, \alpha)$  from (3) and (4), respectively.

*Step 4.* (Compute trajectory) Compute  $\mathcal{T} = \mathcal{T}(v, \alpha; \mathcal{I})$  on the *true* green,  $\mathcal{I}$ .

In Figure 6 we plot the generated pairs of launch velocity and direction, overlaid on the holeout region. For each sub-figure, one can consider the fraction of randomly generated pairs within the holeout region as one-putt probability. The lower panel of Figure 6 contains the one-putt probability from data (solid), from simulation without green reading error (dashed), and from simulation with green reading error (dash-dotted). From the patterns in the data, one observes that downhill putt is harder than uphill putt in terms of one-putt probability. This pattern is consistent with the simulation results with green reading error, but not with the results without green reading error.

## 4. Numerical Results

In the general setting for the numerical experiments in this section, we assume that the speed of green is constant, and it is 11 feet as measured by a Stimpmeter<sup>5</sup>. We use the second order Runge-Kutta method for numerical integration of differential equations, in which a trajectory is computed at discrete points in time with the fixed length of integration interval,  $\Delta t = 0.1$  sec. See

<sup>5</sup>In Section 4.2 we also perform experiments on greens with different speeds, i.e., 8-, 11-, and 14-Stimp greens.

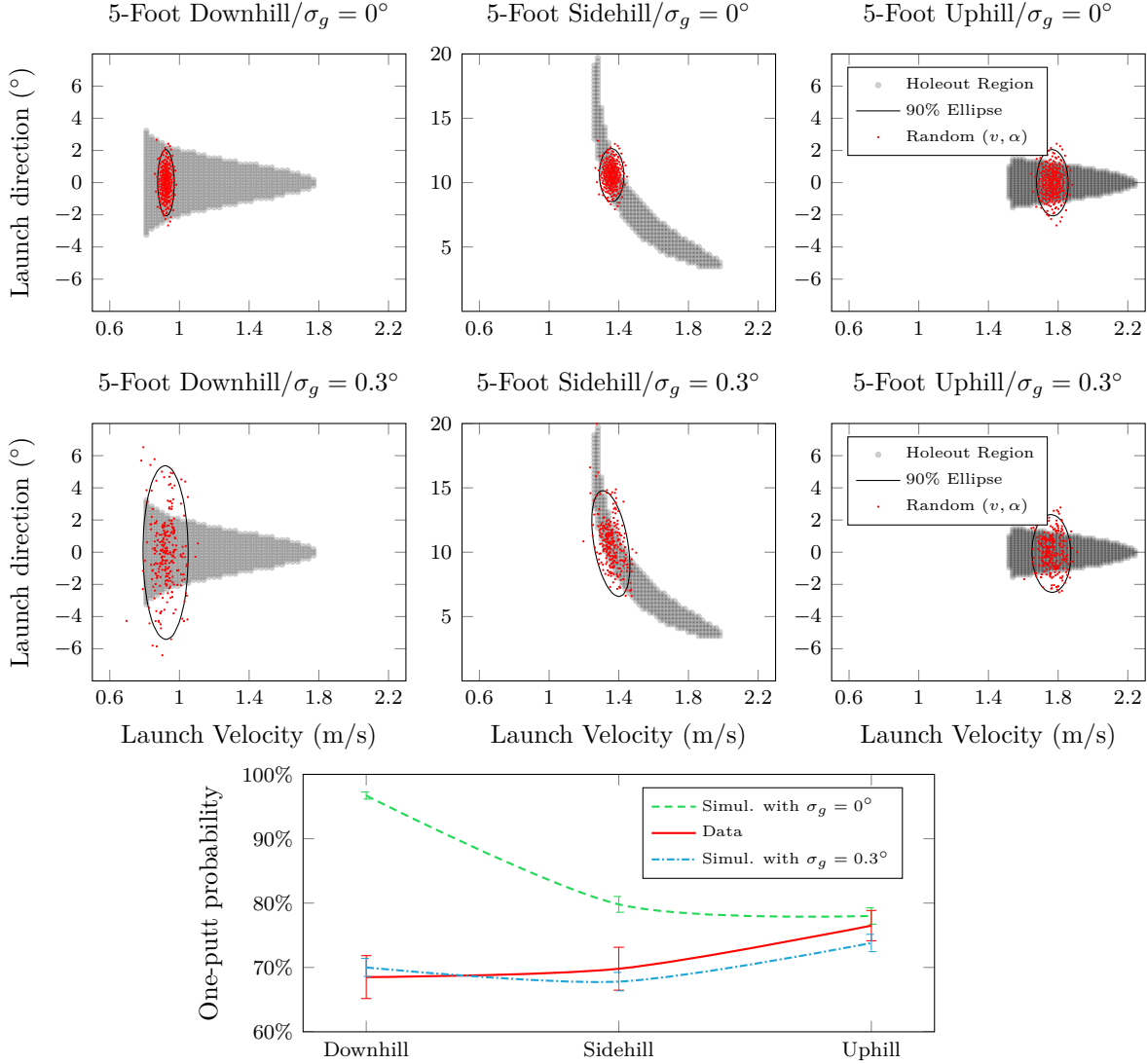


**Figure 6:** The 6 panels with holeout regions contain randomly generated launch velocities and directions for 5-foot downhill, sidehill, and uphill putts on 2.3°-sloped green. The target distance is 1.5 feet for all cases. Each 90% ellipse contains 90% of randomly generated launch velocities and directions. In the upper 3 panels, the simulation parameters are  $(\sigma_g, f(v^2)/v^2, \sigma_\alpha) = (0^\circ, 5\%, 1^\circ)$ , while in the middle 3 panels, the simulation parameters are  $(\sigma_g, f(v^2)/v^2, \sigma_\alpha) = (0.3^\circ, 5\%, 1^\circ)$ . In the lower panel, the error bars indicate 95% confidence intervals about the estimations.

Appendix A.1 for the accuracy and efficiency of numerical integration with this setting. Random variables are generated using the Sobol sequence (Press (2007)) that helps reduce standard errors of estimations. For  $2^{12} - 1 = 4095$  trials for each simulation, the standard error in the average number of putts is always less than 0.0065.

## 4.1. Calibration

Calibration of the model involves estimating the values of model parameters in an attempt to match the performance statistics in the PGA tour data described in Section 2. Specifically, we estimate the skill parameters,  $\sigma = (\sigma_{g1}, \sigma_{g2}, f(\cdot), \sigma_\alpha)$ , and the targeting strategy  $D$ .  $f(\cdot)$  is a piecewise linear function of  $v^2$  with 3 break points at  $v = 1, 2$ , and  $3m/s$ . Therefore, it requires three parameters to describe the function  $f$ . The targeting strategy  $D$  is a vector of  $K + K'$  target distances. The detailed calibration steps will be discussed in the Appendix A.3, and we only sketch the outline in this section.

We consider the three performance statistics; average number of putts, standard deviation of remaining distance, and fraction short. We find the least square estimators of the parameters that minimize the weighted sum of mean-squared errors between the model and the data. Formally, the calibration problem can be formulated as

$$(6) \quad \min_{\sigma \in \Sigma, D \in \mathcal{D}} \hat{J}(\sigma, D) = w_1 \mathbf{mse}_1 + w_2 \mathbf{mse}_2 + w_3 \mathbf{mse}_3,$$

where  $\mathbf{mse}_1$  represents the mean-squared error in average numbers of putts from the model and the data.  $\mathbf{mse}_2$  and  $\mathbf{mse}_3$  are defined similarly for standard deviation of remaining distance and for fraction short, respectively.  $w_1, w_2$ , and  $w_3$  are weights associated to each term.

**Remark 1.** *Bansal and Broadie (2008) calibrates the golfer skill parameters only with respect to average number of putts data, in which case the model is fitted well to the data with a constant target distance. However, in the calibration problem (6), we also consider standard deviation of remaining distance and fraction short as the performance statistics to be matched to the data. This naturally requires the targeting strategy  $D$  to be calibrated as well as the skill parameters, since the two statistics highly depend on the targeting strategy.*

The fitted golfer skill parameters and the target distance from data<sup>6</sup> are given in Figure 7. The root-mean-squared errors are 0.015 in average number of putts, 0.4 feet in standard deviation of remaining distance, and 1.5% in fraction short. Note that the green reading error for the second putt (i.e.,  $\sigma_{g2}$ ) is less than that of the first putt (i.e.,  $\sigma_{g1}$ ). The reduction in the magnitude of green reading error can be explained by the fact that golfers observe the trajectories of the first putts and update their own estimates on the green slope. As can be seen in the lower panel of Figure 7, the target distance inferred from data is not constant, but is rather a function of putt length, angle, and slope.

The patterns in the performance statistics observed from the calibrated model are well-matched to those observed in the data in Section 2. Representatively, see Figure 8 to compare the patterns in average number of putts from the model and the data. The patterns in the fraction short and standard deviation of remaining distance can also be seen in Figures 18-19 in the appendix.

---

<sup>6</sup>We cannot directly observe a target distance in the Shotlink data. Instead, recalling that the performance statistics are functions of target distance, we *infer* the target distance by fitting the performance statistics to data. We call the *target distance from data* as the target distance obtained as a result of the calibration.

Putters	Green Reading Error		Velocity Error( $f(v^2)/v^2$ )			Direction Error
	$\sigma_{g1}$	$\sigma_{g2}$	v=1m/s	v=2m/s	v=3m/s	$\sigma_\alpha$
Best	0.379°	0.272°	1.9%	3.5%	4.4%	0.626°
Average	0.400°	0.303°	3.4%	4.1%	4.3%	0.791°
Worst	0.435°	0.313°	4.6%	5.8%	5.5%	0.903°

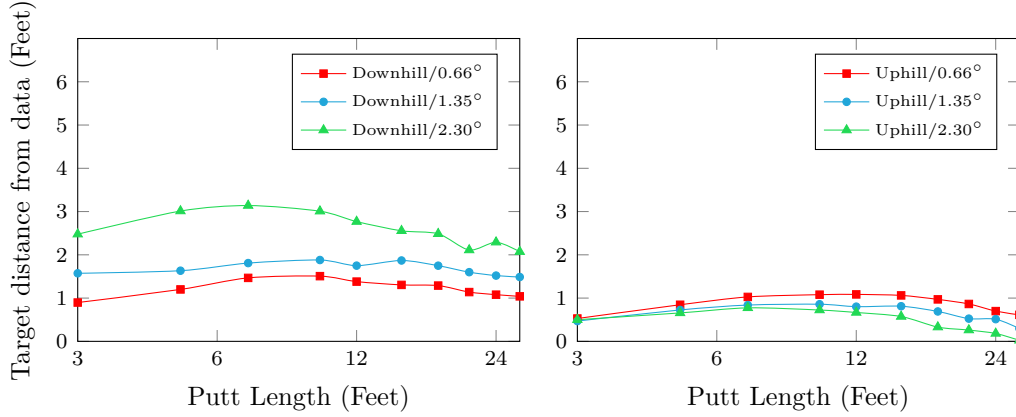


**Figure 7:** The calibration result. The skill parameters are in the upper table and the target distances from data are shown in the lower figures. We provide the fitted golfer skill parameters for best, average, and worst putters, but show the fitted target distance only for the average putter for the matter of limited space. Note that the velocity errors are expressed in relative term,  $f(v^2)/v^2$ , as a percentage, instead of the absolute term,  $f(v^2)$ . The lower figures represent the target distances for the *average* putters.

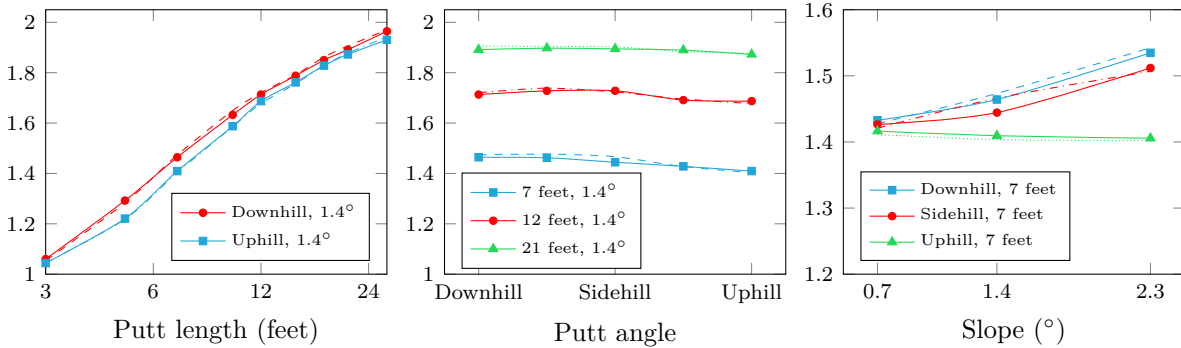


**Figure 8:** Average number of putts from the calibrated model (solid) and from the data (dashed). The overall root-mean-squared error in average number of putts is 0.015.

## 4.2. Optimal Target Distance Past the Hole

Given any putt location  $\mathcal{I}$  and skill parameters  $\sigma$ , we define the optimal target distance as a target distance beyond hole that achieves the lowest *expected* number of putts for holeout. It might seem natural that the better target must be closer to the hole, so that the second putt would be easy when the putt is missed. However, somewhat surprisingly, this is far from the best answer in the presence of physical and green-reading errors. For example, suppose the target distance is 0, i.e., a ball is expected to stop at the hole. In this case, there is a significant chance that the ball is short

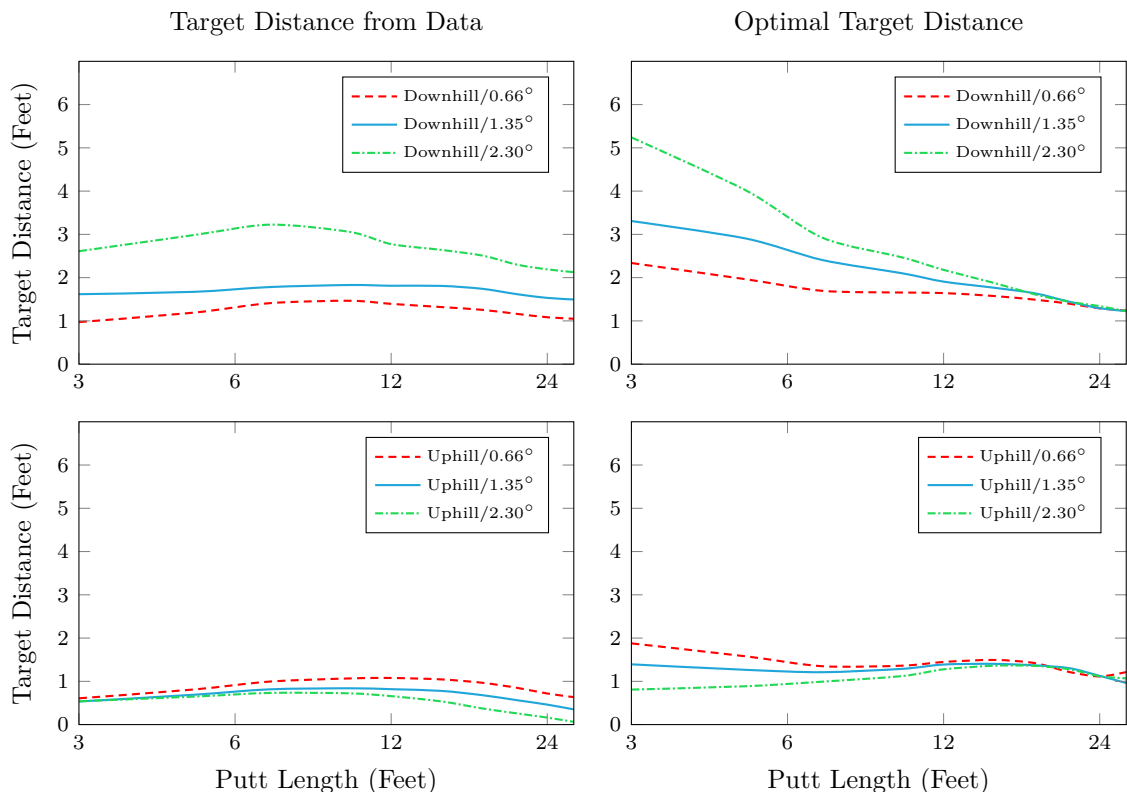


**Figure 9:** The target distances from data on the left column and the optimal target distances on the right column. The target distances from data are the same as those in Figure 7. Both of the target distance from data and the optimal target distance are computed on 11-Stimp green.

to the hole, in which case the number of putts would increase. For another example, suppose the target distance is too far beyond the hole. If the ball misses the hole, it most likely ends far from the hole, in which case the number of putts is likely to increase as well. Therefore, the optimal target distance is the right amount of *excessive* distance beyond the hole, so that not only the chance for holeout is maximized, but also the second putt is easy when the hole is missed.

As mentioned in the previous section, the constant target distance is not optimal. Here is an intuitive explanation why the optimal target distance is not constant. Consider equidistant downhill and uphill putts on the same green. Recall that, with fixed skill levels, the downhill putt is harder than the uphill putt. Therefore, it makes sense that one would want to have the second putt at an *uphill* position, in case the first putt is missed. Therefore, for the downhill putt, an aggressive target would most likely lead the second position at uphill, if it misses the hole. For the uphill putt, a less aggressive target would do so. This is why the optimal target distance is not constant; the optimal targets for downhill putts are generally farther from the hole than those for uphill putts.

Formally, we denote  $d^*(\mathcal{I}; \sigma)$  as the optimal target distance beyond the hole at putt location  $\mathcal{I}$ , given the golfer skill parameter  $\sigma$ . We find the optimal target distances at discrete locations  $I_k$ ,  $k = 1, \dots, K$ . The optimal targeting *strategy* is a vector of the optimal targeting distances, i.e.,

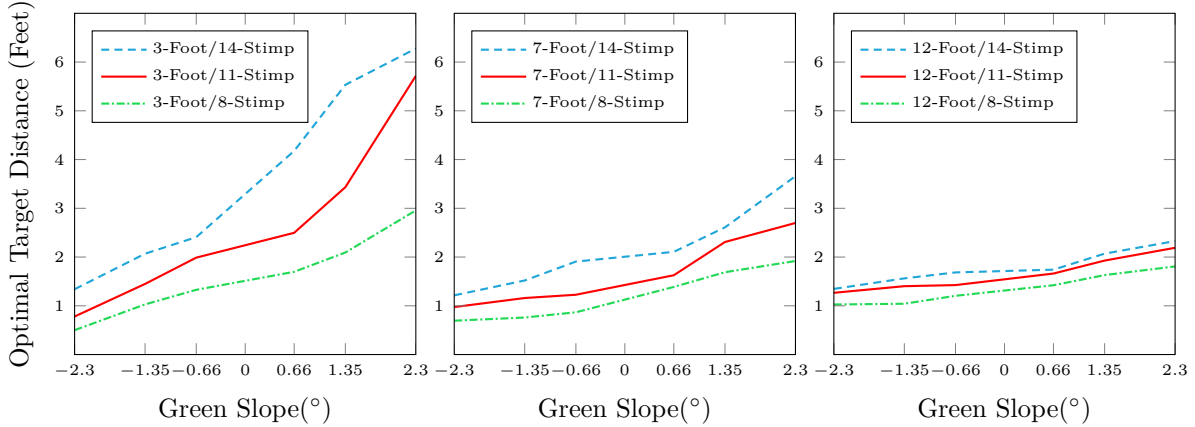


**Figure 10:** Optimal target distance beyond the hole by green slope. The putt angle is fixed to  $18^\circ$ , and thus, positive slopes implies downhill putts and negative slopes implies uphill putts. (In other words, a downhill putt on  $1.35^\circ$  slope is equivalent to an uphill putt on  $-1.35^\circ$  slope.) It can be seen in these figures that, for a fixed putt length, the optimal target distance increases with green slope and green speed. Also, long putts are less sensitive to the green slope and speed than short putts.

$D^*(\sigma) = (d^*(I_1; \sigma), d^*(I_2; \sigma), \dots, d^*(I_K; \sigma)).$ <sup>7</sup> Formally,

$$(7) \quad d^*(I_k; \sigma) = \operatorname{argmin}_{d \in \mathcal{R}^+} J_1(d; \sigma, I_k), \quad \text{for all } k = 1, \dots, K,$$

where  $J_1(d; \sigma, I)$  is the average number of putts as a function of target distance  $d$ , given the skill parameter  $\sigma$  and putt location  $I$ .

The optimal target distances are computed for putt lengths  $\{3, 5, 7, 10, 12, 15, 18, 21, 27\}$  in feet, angles  $\{18^\circ, 90^\circ, 162^\circ\}$ , green slopes  $\{0.66^\circ, 1.35^\circ, 2.30^\circ\}$ , and green speed  $\{8, 11, 14\}$ -Stimp. In Figure 9, we show the optimal target distance by putt length and compare it with the target distance from data. In Figure 10 the optimal target is shown as functions of green slope and speed. For a fixed putt length, the optimal target distance increases with green slope and speed; that is, one should aim aggressively as putt gets harder. Also, one should note that the optimal target distance is more sensitive to green slope and speed for short putts than for long putts; for example, on 11-Stimp green, the optimal target for 3 footer varies from 1 to 6 feet, while the optimal target for 12 footer varies from 1 to 2 feet.

According to our numerical experiment, for 5-foot putts on 11-Stimp green, the average putter in PGA Tournament can save 0.014 putts on average<sup>8</sup> with the optimal target distances. Given that the difference in the average number of putts between the best and average putters is 0.054, the reduction by 0.014 is significant. (See Table 1.)

<sup>7</sup>In this subsection, we only consider the optimal targeting strategy for the first putts. We do not provide details for the second putts since exactly the same analysis would apply.

<sup>8</sup>0.014 is the weighted average of the numbers of putts at 5-foot positions for different putt angles and slopes; the weights are the relative frequencies of each putt angle and slope. Roughly, the decrease in average number of putts by 0.014 corresponds to the increase in one-putt probability by 1.7%.

5-foot		Freq.	Diff. between Avg&Best	Gain due to Opt.Target	Gain/Diff %
Slope(°)	Angle				
0.66°	Downhill	11.8%	0.038	0.009	24%
	Sidehill	13.2%	0.049	0.004	8%
	Uphill	16.5%	0.056	0.004	7%
1.35°	Downhill	12.7%	0.040	0.015	36%
	Sidehill	14.7%	0.082	0.048	58%
	Uphill	26.6%	0.056	0.005	9%
2.30°	Downhill	0.9%	0.044	0.013	30%
	Sidehill	1.0%	0.102	0.056	55%
	Uphill	2.6%	0.048	0.015	32%
All		100.0%	0.054	0.014	26%

**Table 1:** The number of putts gained due to the optimal target for 5-foot putts on 11-Stimp green.  $2^{13} - 1 = 8191$  trials are done for each estimation in the table. The standard error is less than 0.002 in all cases. The last row is averaged with relative frequencies as weights.

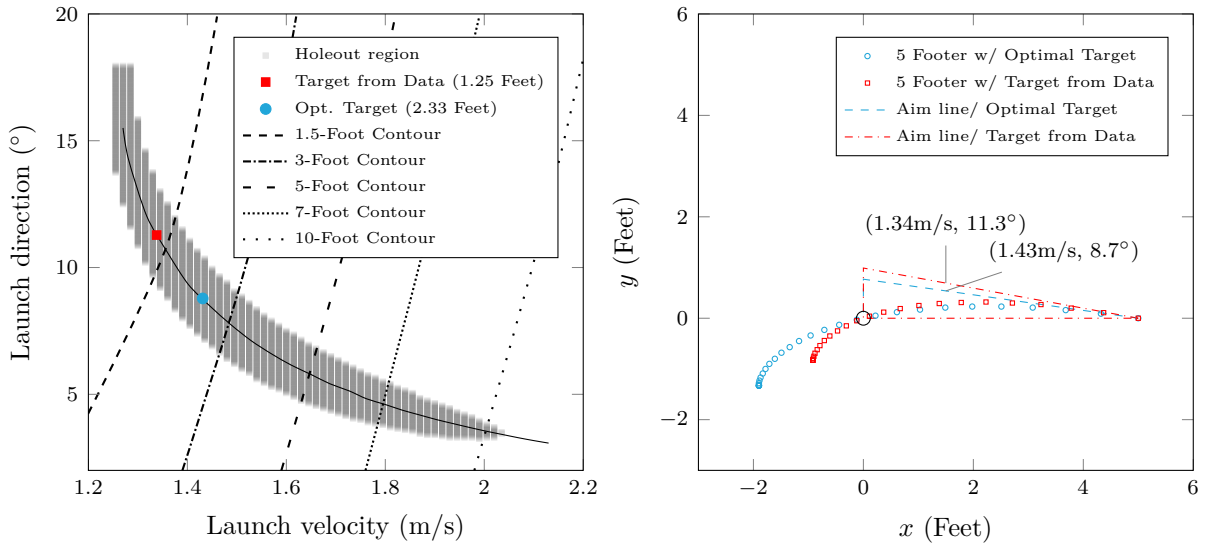


**Figure 11:** The trajectories of 5-foot sidehill putts with the optimal target and the target from data on 2.3° slope green. The optimal target (2.33 feet) is more aggressive than the target from data (1.25 feet).

### 4.3. Attribution Analysis of Putts per Round

The putts per round refers to the total number of putts during a round (18 holes). According to our data, the numbers of putts per round for the best and worst putters are 28.4 and 30.0, respectively. In this section we decompose the differences in putts per round between these groups by four factors; the differences due to green reading error, velocity error, direction error, and fraction short strategy. The first three terms are related to the three golfer skill factors. The fraction short strategy is the targeting strategy *inferred* from the fraction short data and will be explained shortly. Briefly, the best putters have lower fraction short than the worst putters. (See Figure 15.) This in turn implies that the best putters prefer lower fraction short—hence, more aggressive—strategy than the worst putters.

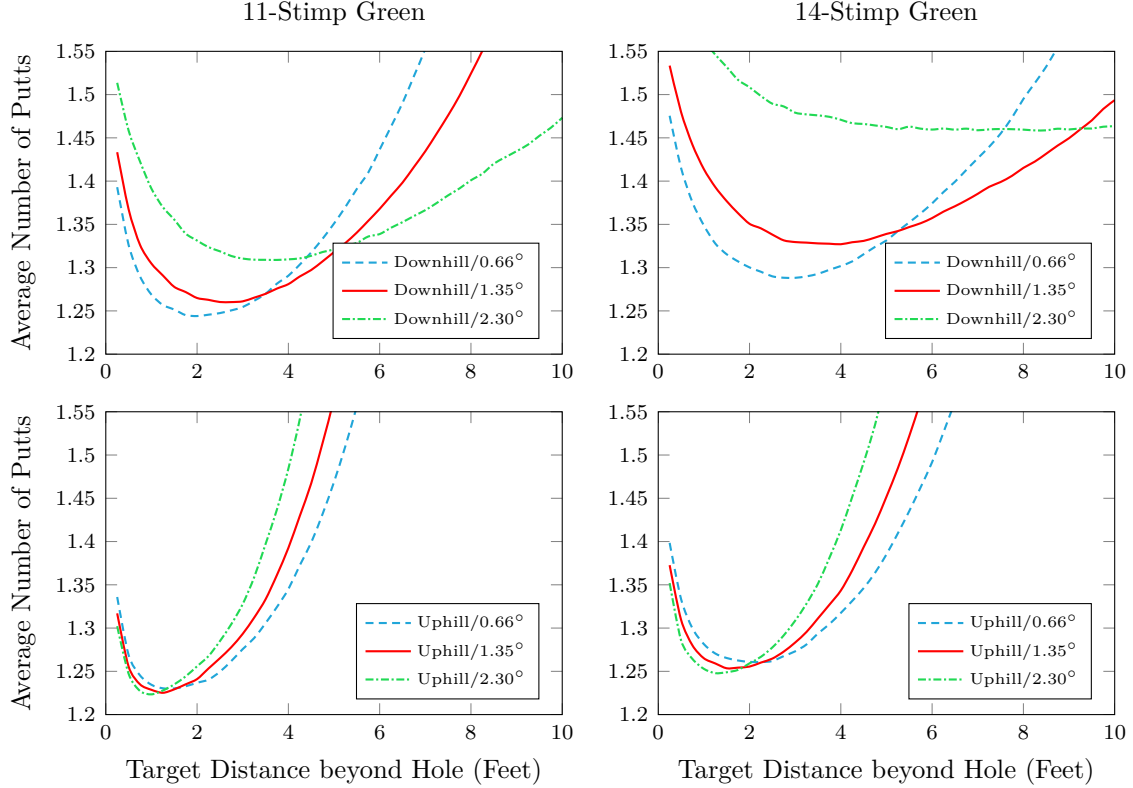


**Figure 12:** Average number of putts by target distance for 5-foot putts. The left panels are the results on 11-Stimp green and the right panels are the results on 14-Stimp green.

We denote  $(\sigma^{\text{best}}, D^{\text{best}})$  and  $(\sigma^{\text{worst}}, D^{\text{worst}})$  as the golfer skill parameters and targeting strategies for the best and worst putters, respectively. To measure what portion of the difference in putts per round between the best and worst putters is attributable to the green reading skill factor, we first estimate putts per round with the worst putter's parameter  $(\sigma^{\text{worst}}, D^{\text{worst}})$ . Then we estimate putts per round with  $(\sigma_{g1}^{\text{worst}}, \sigma_{g2}^{\text{worst}})$  substituted with  $(\sigma_{g1}^{\text{best}}, \sigma_{g2}^{\text{best}})$ , while all the other factors being unchanged. The difference between the two estimates of putts per round is the portion attributable to the green reading factor. Likewise, repeat the similar analysis for velocity and direction factors.

We measure the portion attributable to fraction short strategy in a following way. For fixed skill parameters, a fraction short statistics is exclusively controlled by a targeting strategy, and thus, the difference in putts per round due to the different targeting strategies is approximately equivalent to the difference due to the fraction short strategy. To be specific, we first define  $\hat{D}^{\text{worst}} = (\hat{d}^{\text{worst}}(I_1), \dots, \hat{d}^{\text{worst}}(I_K))$  as the target distances fitted to the fraction short data of the *worst* putters, and  $\hat{D}^{\text{best}} = (\hat{d}^{\text{best}}(I_1), \dots, \hat{d}^{\text{best}}(I_K))$  as the target distances fitted to the fraction short data of the *best* putters. Specifically,  $\hat{D}^{\text{best}}$  and  $\hat{D}^{\text{worst}}$  are target distances fitted only to the fraction short data. These are different from  $D^{\text{best}}$  and  $D^{\text{worst}}$  in Figure 7, which are calibrated to match all the three performance statistics; the average number of putts, fraction short, and standard deviation of remaining distance. Then, with the skill parameter  $\sigma^{\text{worst}}$  fixed, we estimate putts per round of the worst putters, once with  $D^{\text{worst}}$  and then with  $D^{\text{best}}$ . The difference between

Factors	All Putts	by Putt Length	
		Short Putts	Long Putts
Direction Error ( $\sigma_\alpha$ )	38% (4.0%)	44% (4.4%)	31% (3.5%)
Velocity Error ( $f(\cdot)$ )	18% (1.8%)	14% (1.2%)	23% (2.5%)
Green Reading Error ( $\sigma_g$ )	41% (5.0%)	41% (5.0%)	42% (5.1%)
Suboptimal Fraction Short Strategy	3% (0.3%)	1% (0.7%)	4% (0.2%)
Total Difference	1.20	1.32	1.09

**Table 2:** Result of the attribution analysis. For example, the difference in putts per round between best and worst putters is 1.20, of which 38% is due to green reading skill, 41% is due to direction error, 18% is due to velocity error, and the rest 3% is due to suboptimal fraction short strategy. In this table, short (long) putts represents the those with putt length less (greater) than 10 feet. The values in the parenthesis are standard errors (see Remark 2).

these two estimates of the putts per round is the portion attributable to the suboptimal fraction short strategy.

The result of the attribution analysis is presented in Table 2. The direction control and green reading abilities are the major factors that distinguish the best and worst putters, while the distance control abilities (i.e., velocity control ability and fraction short strategy) are relatively minor. Further, we break them down by putt length; short putts ( $\leq 10$  feet) and long putts ( $> 10$  feet). It can be seen that the direction (resp., velocity) control ability is more (resp., less) critical for short putts than long ones, although the impact of velocity control ability is still less compared to the direction control and green-reading abilities.

**Remark 2 (Robustness of the attribution analysis).** *In the calibration process, close examination of the relationship between the objective function in (6) and the golfer skill parameters  $\sigma = (\sigma_{g1}, \sigma_{g2}, f(\cdot), \sigma_\alpha)$  reveals that the objective function is sensitive not only to each parameter individually, but also to the combination of these parameters. Thus, there are more than one set of golfer skill parameters that are very close to the optimum. For instance, if we fix one of these parameters, say,  $\sigma_\alpha$ , then we can use the other parameter, say,  $\sigma_{g1}$ , so that the objective function remains close to the optimal value. This implies one can expect the range of the optimal set of parameters rather than a unique optimum. Thus, for the more robust attribution analysis, we repeat the calibration for the best, average, and worst putters for 10 random subsets of the data. By doing so, we get estimation error of each of the four attribution terms.*

## 5. Concluding Remarks

Our research starts with the statistical analysis on the putting performance data, provides the random putting model for the putting, and calibrates it to the data. Also, we have shown by numerical experiments that one can significantly lower the number of putts by targeting more aggressively, without improving the skill levels. Another inference from the numerical experiments is the attribution analysis, in which we have shown that the key factors that separate the best and worst putters are the direction control and green reading abilities.

We outline several future research directions of the putting model. (a) We have made various special assumptions in this analysis, and further research ought to extend the basics here. (b) One direction along the line of green-reading model is to look at the green-updating model in detail. Our model does not explain how the green slope estimate is updated for second putts, and it would be interesting to take, for example, a Bayesian approach to model the green-updating scheme. This means that the green slope estimate for the first putt could be considered as a prior and the trajectories on the same green could be considered as observations (with some noise). With the prior and the observations, the posterior distribution could be established, i.e. the distribution for the green slope estimate for second putt.

## References

- Matulya Bansal and Mark Broadie. A simulation model to analyze the impact of hole size on putting in golf. In *Simulation Conference, 2008. WSC 2008. Winter*, pages 2826–2834. IEEE, 2008.
- Mark Broadie. Assessing golfer performance using golfmetrics. In *Science and golf V: Proceedings of the 2008 world scientific congress of golf*, pages 253–262, 2008.
- Mark Broadie. Assessing golfer performance on the pga tour. *Interfaces*, 42(2):146–165, 2012.
- Andrew Gelman and Deborah Nolan. A probability model for golf putting. *Teaching statistics*, 24(3):93–95, 2002.
- Brian W Holmes. Putting: How a golf ball and hole interact. *American Journal of Physics*, 59(2):129–136, 1991.
- D Pelz. Putting bible: the complete guide to mastering the green. *Publication Doubleday, New York*, 2000.
- AR Penner. The physics of putting. *Canadian journal of physics*, 80(2):83–96, 2002.
- Scott K Perry. The proof is in the putting. *The Physics Teacher*, 40(7):411–414, 2002.
- William H Press. *Numerical recipes 3rd edition: The art of scientific computing*. Cambridge university press, 2007.
- Robert J Vanderbei. A case study in trajectory optimization: Putting on an uneven green. *SIAG/OPT Views-and-News*, 12(1):6–14, 2001.

## A. Appendix

In this section we discuss some issues on the efficiency and accuracy of the numerical integration routines (A.1). Also, we provide an approximate method to estimate the average number of putts and putts per round in Section A.2 and present details on the calibration method in Section A.3.

### A.1. Numerical Integration of Differential Equations of Motion

In this subsection we overview the differential equations of motion given in Penner (2002) and discuss some numerical integration techniques. The equations for a trajectory of a golf ball are derived in Penner (2002) so we will omit the detail. Yet, we introduce a numerical integration routine called the Runge-Kutta method, and analyze the accuracy and the efficiency of the routine. In this paper, we calculate millions of trajectories during simulation, hence, the parameters of the routine need to be tuned so that we can achieve *balanced* accuracy and efficiency.

We use slightly different notations than those in Penner's paper. Let  $f_r$  be the retarding force due to the deformed surface and  $\phi$  be the angle w.r.t. the y-axis. The velocity of a ball is denoted as  $v$  and its angle w.r.t. the y-axis is denoted as  $\beta$ . The golf ball has mass  $m$  and radius  $R$ , and we denote  $I_b$  as the moment of inertia of the golf ball, which is  $2/5$  since it is a uniform solid sphere.  $\rho_g$  is the coefficient of the retarding force. The green slope is  $\theta$  along the x-axis and  $\varphi$  along the y-axis. The equations of motion of a ball are the following second order ordinary differential equations,

$$(8) \quad \begin{aligned} m\ddot{x} &= -mg \sin \theta - f_r \sin \phi \\ m\ddot{y} &= -mg \cos \theta \sin \varphi - f_r \cos \phi, \end{aligned}$$

where the frictional force  $f_r$  and its angle  $\phi$  are defined as

$$(9) \quad \begin{aligned} f_r &= \frac{\rho_g \cos \theta \cos \varphi \cos \beta - I_b \cos \theta \sin \varphi}{(1 + I_b) \cos \phi} mg \\ \tan \phi &= \frac{\rho_g \cos \theta \cos \varphi \sin \beta - I_b \sin \theta}{\rho_g \cos \theta \cos \varphi \cos \beta - I_b \cos \theta \sin \varphi}. \end{aligned}$$

Then, starting at the initial position  $(x, y)$  with the launch velocity and direction  $(\dot{x}, \dot{y}) = (v_x, v_y)$  at  $t = 0$ , we march forward by computing differentials,  $\Delta x$ ,  $\Delta y$ ,  $\Delta \dot{x}$ , and  $\Delta \dot{y}$ , at each step. We use the 2nd order Runge-Kutta method to calculate the differential terms. (See Press (2007).) Denote  $(x_n, y_n)$  as the position at time  $t_n = n\Delta t$ . The below equations show how the differential terms are updated at each step in the 2nd order Runge-Kutta method.

$$(10) \quad \begin{aligned} (k1, k2, k3, k4) &= \Delta t \cdot h(x_n, y_n, \dot{x}_n, \dot{y}_n), \\ (t1, t2, t3, t4) &= \Delta t \cdot h(x_n + \frac{1}{2}k1, y_n + \frac{1}{2}k2, \dot{x}_n + \frac{1}{2}k3, \dot{y}_n + \frac{1}{2}k4), \\ (x_{n+1}, y_{n+1}, \dot{x}_{n+1}, \dot{y}_{n+1}) &= (x_n, y_n, \dot{x}_n, \dot{y}_n) + (t1, t2, t3, t4) + O(\Delta t^3), \end{aligned}$$

where  $h(x_n, y_n, \dot{x}_n, \dot{y}_n) = (\dot{x}_n, \dot{y}_n, \ddot{x}_n, \ddot{y}_n)$ . Note that the 2nd order Runge-Kutta method takes

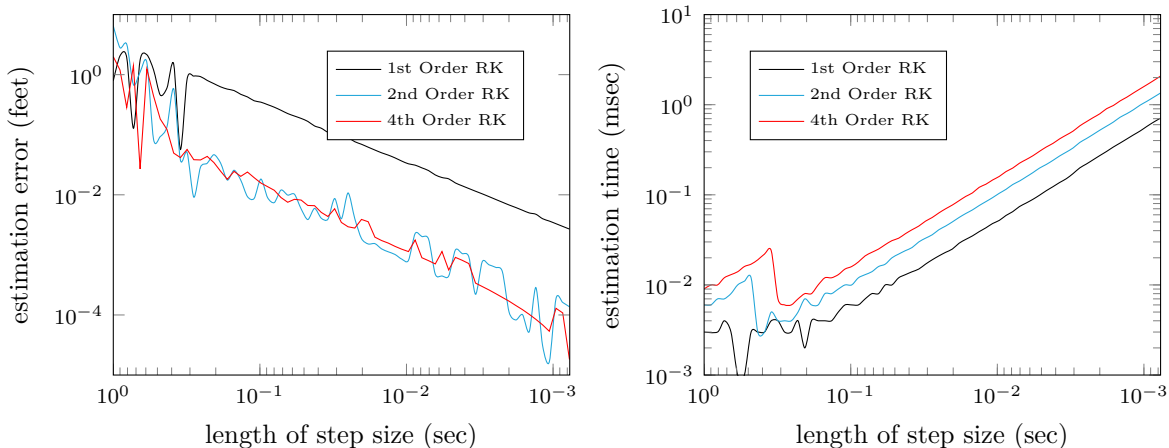


**Figure 13:** The estimation errors (left) for different orders of Runge-Kutta methods in estimating the end points (feet) for 10-foot downhill putt. There is a noticeable improvement from the first order to the second order Runge-Kutta method, but no significant improvement in accuracy for the fourth order method. The estimation time (right) is the cpu time required to compute 100 same trajectories, measured in milliseconds.

derivatives twice; once at the initial point and then at the midpoint.

The efficiency of Runge-Kutta method depends on the order of integration. Note that higher order gives the higher accuracy in general, but surely not always. The first order Runge-Kutta method is the simplest (and least accurate) method that takes derivative at an initial point only. The fourth order Runge-Kutta method takes four derivatives: once at an initial point, twice at trial midpoints, and once at an end point. It turned out that the second order Runge-Kutta method fits for our purpose since it efficiently balances the accuracy and the computational burden; it is as accurate as the fourth order Runge-Kutta method, but has shorter estimation time. See Figure 13 that compares the estimation errors in putt distance by the first, second, and fourth order Runge-Kutta methods. In the figure, each estimation error is calculated with respect to sufficiently accurate estimation with  $\Delta t = 0.00001$ sec using the fourth order Runge-Kutta method. The numerical integration results in Figure 13 were run on 64-bit operating system with 2.80GHz professor and 4GB RAM.

## A.2. Estimation of Average Number of Putts and Putts per Round

The estimation of performance statistics, such as one-putt probability, fraction short, and standard deviation of remaining distance, via simulation is straightforward. They are simply estimated by generating  $N$  sample trajectories and taking averages (or standard deviations) over those trajectories.

However, the estimation of the average number of putts is not as straightforward as the above performance measures since, for each simulation trial, a sequence of trajectories should be generated until the ball is sunk. To be specific, let  $\mathcal{I}$  and  $\mathcal{I}'$  be the initial and the second putt locations. Define  $J_1 \equiv J_1(\sigma, d(\mathcal{I}); \mathcal{I})$  as the number of putts for skill parameter  $\sigma$  and target distance  $d(\mathcal{I})$ ,

given the initial location  $\mathcal{I}$ . It is a random variable since trajectory is random. If the first putt is holeout,  $\mathcal{I}'$  is exactly the hole position and  $J_1(\sigma, d(\mathcal{I}); \mathcal{I}) = 1$ . If not, another putt that starts at  $\mathcal{I}'$  should be generated. Thus, the number of putts at  $I$  is estimated via recursive simulation:

$$J_1(\sigma, d(\mathcal{I}); \mathcal{I}) = 1 + J_1(\sigma, d(\mathcal{I}'); \mathcal{I}').$$

The nested structure causes a computational challenge, so we introduce an alternative approach by combining simulation model for the first putts and the data for the second and later putts.

Define  $p_1(\mathcal{I})$  as one-putt probability of the first putt *from data* at  $\mathcal{I}$  and  $\hat{p}_1(\sigma, d(\mathcal{I}); \mathcal{I})$  as its estimation *by simulation* method with golfer skill parameter  $\sigma$  and target distance  $d(\mathcal{I})$ . Likewise, define  $q_1(\mathcal{I}')$  and  $\hat{q}_1(\sigma, d(\mathcal{I}'); \mathcal{I}')$  as the one-putt probability of the second putt *from data* and *from simulation*, respectively. We assume that the probabilities of more than four putts are negligible. To estimate the average number of putts, first generate  $N$  trajectories to obtain the estimation of  $\hat{p}_1(\sigma, d(\mathcal{I}); \mathcal{I})$  and their second putt locations  $\mathcal{I}'_i, i = 1, \dots, N$ . Then, instead of simulating for  $\hat{q}_1(\sigma, d(\mathcal{I}'), \mathcal{I}'_i)$ , we get  $q_1(\mathcal{I}'_i)$  from data by interpolating one-putt probabilities at discrete putt locations,  $\{\mathcal{I}'_k; k = 1, \dots, K'\}$ . Then, the estimation of  $J_1$  is approximated by  $\hat{J}_1$ :

$$(11) \quad \begin{aligned} \hat{J}_1(\sigma, D; \mathcal{I}) = & \hat{p}_1(\sigma, d(\mathcal{I}); \mathcal{I}) + \\ & 2(1 - \hat{p}_1(\sigma, d(\mathcal{I}); \mathcal{I})) \sum_{i=1}^N q_1(\mathcal{I}'_i) + \\ & 3(1 - \hat{p}_1(\sigma, d(\mathcal{I}); \mathcal{I})) \sum_{i=1}^N (1 - q_1(\mathcal{I}'_i)). \end{aligned}$$

In the approximation  $\hat{J}_1$ , only the first putt is generated for each simulation trial and the results for the second and the later putts are inferred from data. This significantly reduces the computational burden of the recursive simulation.

The putts per round is the total number of putts in a round (18 holes). Denote the putts per round as the capital  $M \equiv M(\sigma, D)$ , where  $D = (d(I_1), \dots, d(I_K), d'(I'_1), \dots, d'(I'_K))$  is the target distance vector. The putts per round is approximated as the weighted average of  $\hat{J}_1$ 's at different locations:

$$(12) \quad \hat{M}(\sigma, D) = (1 - \epsilon_0) \frac{18}{K} \sum_{k=1}^K u_k \hat{J}_1(\sigma, d(I_k); I_k),$$

where  $u_k$  is the relative frequency of putts at  $I_k$  from data (Section 2) and  $\epsilon_0$  is the fraction of zero-putt greens. We infer from data that the fraction of zero-putt greens is 1.2%; i.e., we set  $\epsilon_0 = 0.012$ .

### A.3. Calibration Method

The objective of the calibration is to minimize the weighted sum of mean-squared errors in average number of putts, fraction short, and standard deviation of remaining distance. The decision variables are the skill parameters  $\sigma = (\sigma_{g1}, \sigma_{g2}, f(\cdot), \sigma_\alpha)$ , and target distances strategy  $D = (d(I_1), \dots, d(I_K), d'(I'_1), \dots, d'(I'_K))$ . As mentioned in Section 4.1, the simulation parameters are 6-dimensional, since it requires three parameters to characterize the piecewise linear function  $f(\cdot)$ . The dimension of target distance  $D$  depends on the number of putt locations,  $I_1, \dots, I_K$ , and thus, it is high dimensional. The high dimensionality of  $D$  makes the calibration problem computationally hard, so we suggest an alternative approach.

Define  $\hat{J}_1(\sigma, d(\mathcal{I}); \mathcal{I})$  as the average number of putts for the skill parameter  $\sigma$  and the target distance  $d(\mathcal{I})$ , given the putt location  $\mathcal{I}$ . Similarly, define  $\hat{J}_2(\cdot)$  and  $\hat{J}_3(\cdot)$  as the estimations of standard deviation of remaining distance and fraction short, respectively. Denote  $J_1(\cdot)$ ,  $J_2(\cdot)$ , and  $J_3(\cdot)$  as corresponding values inferred from data. The prime symbol on any variable implies it is for the second putt. The calibration problem can be formulated as follows:

$$\begin{aligned}
 \min_{\sigma \in \Sigma, D \in \mathcal{D}} \hat{L}(\sigma, D) &= w_1 \hat{L}_1(\sigma, D) + w_2 \hat{L}_2(\sigma, D) + w_3 \hat{L}_3(\sigma, D) \\
 (13) \quad &= w_1 \left[ \sum_{k=1}^K \left[ \hat{J}_1(\sigma, d(I_k); I_k) - J_1(I_k) \right]^2 + \sum_{k=1}^{K'} \left[ \hat{J}'_1(\sigma, d'(I'_k); I'_k) - J'_1(I'_k) \right]^2 \right] + \\
 &w_2 \left[ \sum_{k=1}^K \left[ \hat{J}_2(\sigma, d(I_k); I_k) - J_2(I_k) \right]^2 + \sum_{k=1}^{K'} \left[ \hat{J}'_2(\sigma, d'(I'_k); I'_k) - J'_2(I'_k) \right]^2 \right] + \\
 &w_3 \left[ \sum_{k=1}^K \left[ \hat{J}_3(\sigma, d(I_k); I_k) - J_3(I_k) \right]^2 + \sum_{k=1}^{K'} \left[ \hat{J}'_3(\sigma, d'(I'_k); I'_k) - J'_3(I'_k) \right]^2 \right],
 \end{aligned}$$

where  $w_1$ ,  $w_2$ , and  $w_3$  are some positive weights. Note that the first sum in each bracket is the mean-squared error for first putts and the second sum is the mean-squared error for second putts. (13) is not an easy problem to solve because of the high dimensionality of  $D$ , however, it can be efficiently solved by dividing it into two phases.

Suppose we are given an initial target distance vector  $D^0$ . Consider the two phases as follows:

**(phase 1)**  $\sigma^1 = \underset{\sigma \in \Sigma}{\operatorname{argmin}} \hat{J}(\sigma, D^0)$ , for fixed  $D^0$ .

**(phase 2)**  $D^1 = \underset{D \in \mathcal{D}}{\operatorname{argmin}} \hat{J}(\sigma_1, D)$ , for fixed  $\sigma^1$ .

The phase 1 is 6-dimensional stochastic approximation problem that can be efficiently solved by any stochastic approximation methods, e.g., Response Surface Methodology (RSM). The phase 2 is a  $(K + K')$ -dimensional stochastic approximation problem, but can be separated into  $K + K'$  number of one-dimensional problems since the objective function is *separable*. To be specific, consider the modified phase 2:

**(phase 2)'** For fixed  $\sigma^1$  and for each first putt location  $I_k$ ,  $k = 1, 2, \dots, K$ , solve

$$d(I_k) \equiv \operatorname{argmin}_{d \in \mathcal{R}^+} w_1 \left[ \hat{J}_1(\sigma, d; I_k) - J_1(I_k) \right]^2 + w_2 \left[ \hat{J}_2(\sigma, d; I_k) - J_2(I_k) \right]^2 + w_3 \left[ \hat{J}_3(\sigma, d; I_k) - J_3(I_k) \right]^2.$$

Likewise, for each second putt location  $I'_k$ ,  $k = 1, 2, \dots, K'$ , solve

$$d'(I'_k) \equiv \operatorname{argmin}_{d \in \mathcal{R}^+} w_1 \left[ \hat{J}_1(\sigma, d; I'_k) - J_1(I'_k) \right]^2 + w_2 \left[ \hat{J}_2(\sigma, d; I'_k) - J_2(I'_k) \right]^2 + w_3 \left[ \hat{J}_3(\sigma, d; I'_k) - J_3(I'_k) \right]^2.$$

We repeat the above procedures until the objective function  $\hat{L}$  is less than the tolerance level  $\epsilon$ :

*Step 0.* Set  $D = D^0$  and  $i = 1$ .

*Step 1.* Solve (phase 1) to get  $\sigma^i$  for fixed  $D = D^{i-1}$ .

*Step 2.* Solve (phase 2) to get  $D^i$  for fixed  $\sigma = \sigma^i$ .

*Step 3.* If  $\hat{L}(\sigma^i, D^i) \leq \epsilon$ , stop the procedure. Otherwise, let  $i \leftarrow i + 1$  and repeat from *Step 1*.

It remains to discuss the choice of the weights in the objective function,  $w_1$ ,  $w_2$ , and  $w_3$ . It is important to note that the units of the three performance statistics are different; average number of putts and fraction short are no-unit measures, whereas standard deviation of remaining distance is measured in feet. In this paper we use  $(w_1, w_2, w_3) = (0.64, 0.0001, 0.16)$ ; with these weights, the ratios,  $\hat{L}_i/(\hat{L}_1 + \hat{L}_2 + \hat{L}_3)$  in (13) are 60%, 10%, and 30% for  $i = 1, 2, 3$ , respectively.

The results in Section 4.1 are obtained by repeating the above two-stage procedure until the objective value (weighted sum of mean-squared errors) is less than  $\epsilon = 0.0003$ , which required three iterations of the two-stage procedure. We ran the calibration on Columbia Business school's shared cluster, in which we can distribute the computational workload to 15 machines. Each machine has eight 2.4 GHz CPUs. In this setting, it takes about 60 hours for the entire calibration process.

#### A.4. Additional Figures

We present some additional figures in this subsection. To be specific, in Figure 14 we compare the average numbers of putts for the first and the second putts. In Figure 15 we compare the performance statistics between the best and the worst putters. Figure 16 and Figure 17 show fraction short and standard deviation of remaining distance data for the average putters. Lastly, in Figure 18 and Figure 19, we compare the fraction short and the standard deviation of remaining distance from the calibrated model with those in the data.

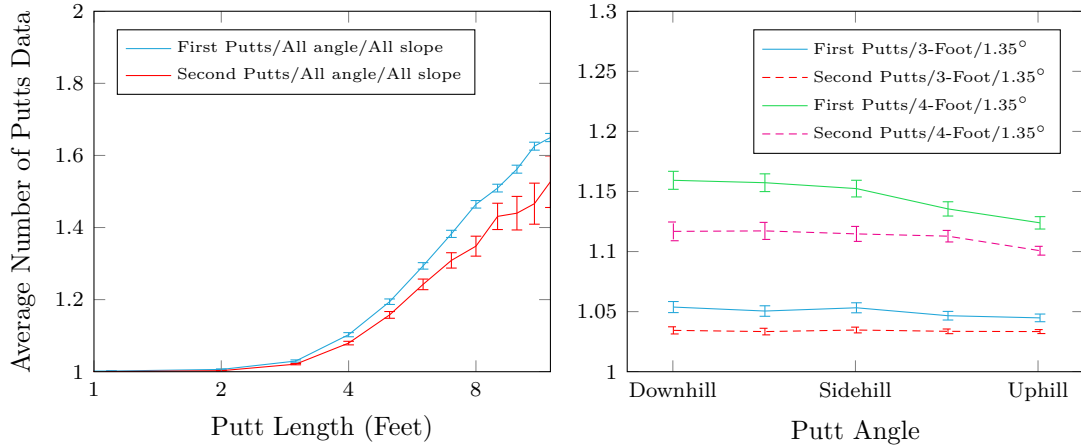


**Figure 14:** First (solid) v.s. second (dotted) putts. The average number of putts for first and second putts are shown as a function of putt length (left) and as a function of putt angle (right). In the left panel, the average number of putts data are averaged over putt angle and slope for each putt length. Each error bar represents 95% confidence interval about each estimation.

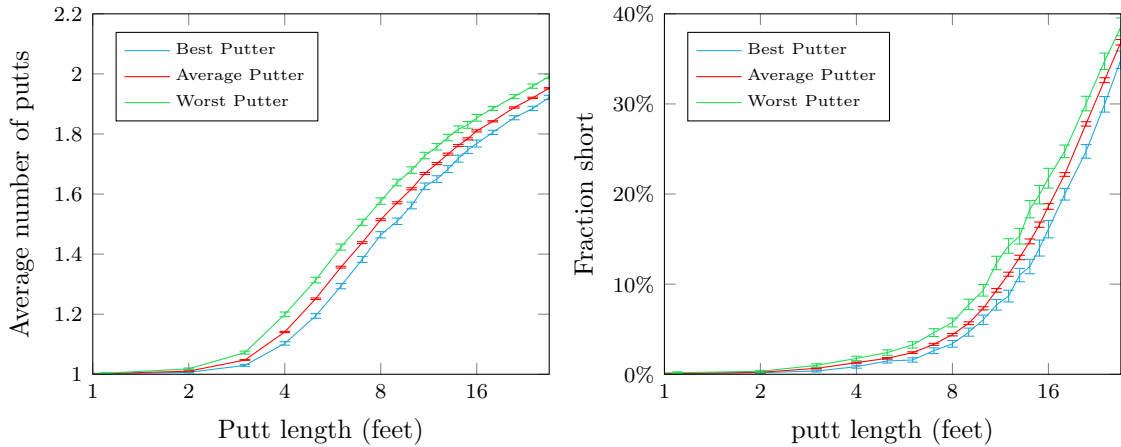


**Figure 15:** Best vs. Worst putters. The left panel is the average number of putts data and the right panel is the fraction short data. The data are displayed as a function of putt length; for each putt length, the data are averaged over all slopes and angles. Each error bar represents 95% confidence interval about each estimation.

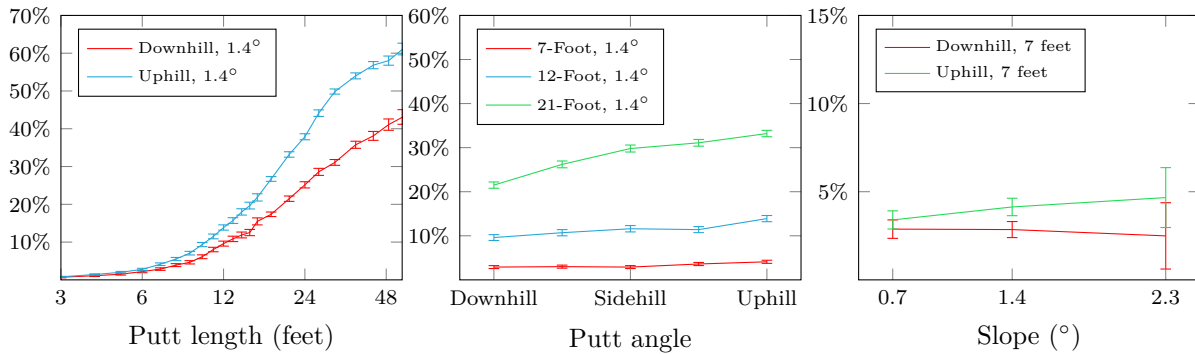


**Figure 16:** Fraction short data for *average* putters. Each error represents 95% confidence interval about each estimation.

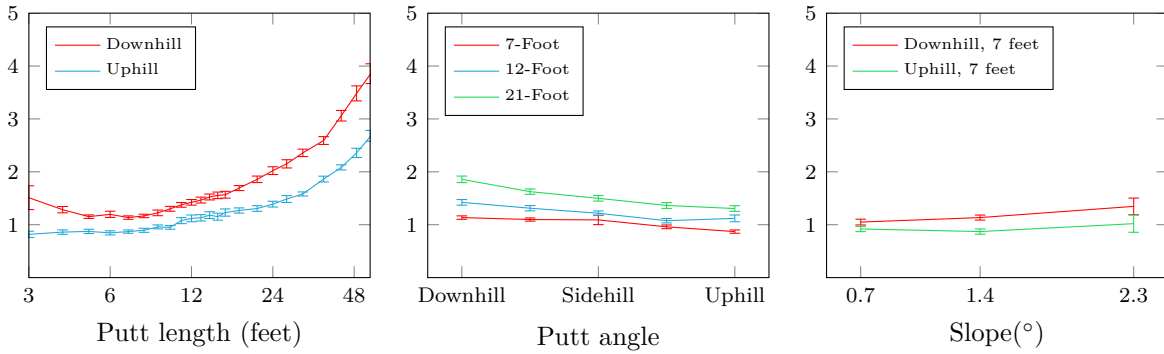


**Figure 17:** Standard deviation of remaining distance data for *average* putters. Each error bar represents 95% confidence interval about each estimation.

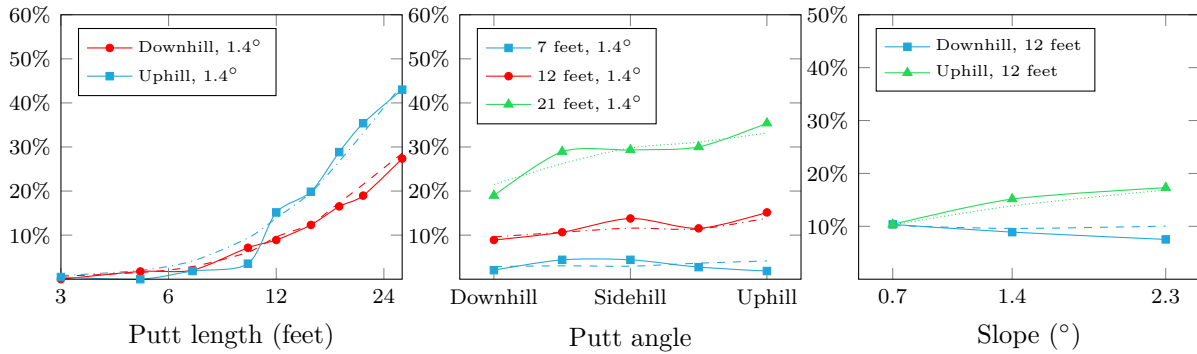


**Figure 18:** Fraction short from the calibrated model (solid) and from the data (dashed). The overall root-mean-squared error in fraction short is 1.5%.

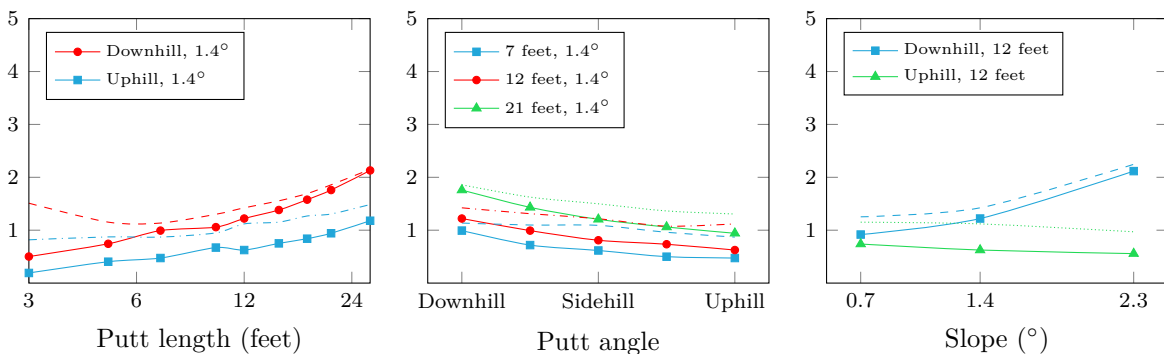


**Figure 19:** Standard deviation of remaining distance from the calibrated model (solid) and from the data (dashed). The overall root-mean-squared error in standard deviation of remaining distance is about 0.4 feet.